



Aza-crown ether derivatives based on stilbene: Two-photon absorption and bioimaging



Wei Li^a, Mingdi Yang^{a,b,*}, Linpan Wang^c, Weiju Zhu^a, Lina Ye^a, Jieying Wu^a, Yupeng Tian^a, Hongping Zhou^{a,*}

^a College of Chemistry and Chemical Engineering, Anhui University and Key Laboratory of Functional Inorganic Materials Chemistry of Anhui Province, 230601 Hefei, PR China

^b School of Materials and Chemical Engineering, Anhui Jianzhu University, Hefei 230601, PR China

^c Department of Civil Engineering, Anhui Vocational and Technical College, 230051 Hefei, PR China

ARTICLE INFO

Article history:

Received 30 January 2014

Received in revised form

23 March 2014

Accepted 25 March 2014

Available online 3 April 2014

Keywords:

Aza-crown ether

Stilbene

SPEF

δ

Bioimaging

TPFM

ABSTRACT

Two novel aza-crown ether derivatives based on stilbene were synthesized and characterized. Their linear photophysical properties were systematically investigated in various solvents. The nonlinear photophysical properties were investigated by two-photon induced fluorescence method. The two-photon absorption cross sections values measured by two-photon excited fluorescence were determined to be 328.2 GM and 246.55 GM for the dyes derived from monoaza 15-crown-5 and 18-crown-6, respectively, which accorded with dipole moment changes under photoexcitation. In addition, a single-photon fluorescence cell imaging experiment proved that dye derived from monoaza 15-crown-5 was suitable for biomedical imaging.

© 2014 Published by Elsevier Ltd.

1. Introduction

The development of materials displaying two-photon absorption (2PA) [1] has attracted great interest in past decades due to a variety of potential applications in photonics and optoelectronics, such as three-dimensional optical data storage, fluorescence imaging, optical limiting, up-converted lasing and microfabrication [2].

The applications of 2PA materials stimulated substantial research on structure-property relationship [3]. The significant issue is how to synthesize the materials with large 2PA cross sections. Some efficient molecular design strategies were put forward to provide guidelines for the development of materials with large two-photon absorption cross sections (σ), including donor–acceptor–donor (D–A–D)-type molecules, donor– π –acceptor (D– π –A)-type molecules, donor– π –donor (D– π –D)-type molecules,

macrocycles, dendrimers, polymers, and multi-branched molecules. Reinhardt synthesized a variety of donor– π –acceptor (D– π –A) and donor– π –donor (D– π –D) derivatives, in which fluorene, biphenyl, or naphthyl groups are employed as the mobile π -electron bridge, and showed that the TPA cross sections become larger if a planar fluorene was used as the π -center [4]. The TPA properties of fluorene derivatives were subsequently optimized by Belfield by introducing a variety of donors and acceptors [5]. The important role of the π -center for the design of large TPA dyes was demonstrated by Prasad, who showed that the TPA cross sections of the D– π –D chromophores based on dithienothiophene as the π -center were larger by an order of magnitude than those of the fluorene derivatives [6]. By combining synthesis, characterization, and theory, Marder, Perry, and Webb found that bis(styryl)-benzene derivatives with donor–acceptor–donor (D–A–D) and acceptor–donor–acceptor (A–D–A) structural motifs, which were linear quadrupolar molecules, showed exceptionally large TPA cross sections [7].

Most organic dyes with large conjugated structures have a major defect that solubility is poor for bioimaging, as a result, it is necessary to enhance their biocompatibility by optimizing the

* Corresponding authors. College of Chemistry and Chemical Engineering, Anhui University and Key Laboratory of Functional Inorganic Materials Chemistry of Anhui Province, 230601 Hefei, PR China. Tel.: +86 551 63861279; fax: +86 551 63861259. E-mail addresses: zhpzhp@263.net, zhouhongping@ahu.edu.cn (H. Zhou).

structure [8]. In the design of the target molecules, the aza-crown ether often used as phase transfer catalyst was introduced. The aza-crown ether serves as the electron donor, meanwhile, it was also expected to endow the molecules hydrophilia. And that crown ether compounds having good solubility and environmental stability are also multidentate ligands that exhibit selectivity for specific metal ions in solutions containing other chemically similar ions, which can be applied to identify ions. In this paper, we designed and synthesized two novel aza-crown ether derivatives-based TPA dyes with dumbbell-shape (D- π -D), aza-crown ether as electron donor and stilbene as the conjugated chain. Compared with simple dimethyl amino substituents, the two dyes showed the similar two-photon absorption property and better solubility. Furthermore, a single-photon fluorescence cell imaging experiment proved the suitability of dye 1 for biomedical imaging.

2. Experimental section

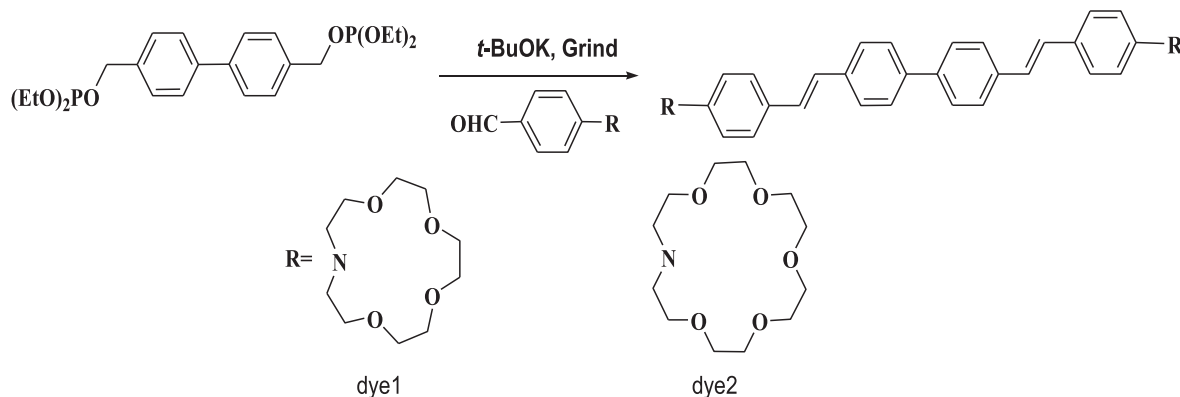
2.1. Apparatus and materials

Chemicals were purchased and used as received. Every solvent was purified by conventional methods beforehand. IR spectra were recorded with a Nicolet FT-IR NEXUS 870 spectrometer (KBr discs) in the 4000–400 cm^{-1} region. ^1H NMR and ^{13}C NMR were recorded on 400 MHz and 100 MHz NMR instruments using CDCl_3 as solvent respectively. The mass spectra were obtained on a Bruker Autoflex III smartbeam mass spectrometer and a Finnigan LCQ Spectrometer. Elemental analyses data were measured by a Perkin Elmer 240B elemental analyzer. The one-photon absorption (OPA) spectra were recorded on a SPECORD S600 spectrophotometer. The one-photon excited fluorescence (OPEF) spectra measurements were performed using a Hitachi F-7000 fluorescence spectrophotometer. For time-resolved fluorescence measurements, the fluorescence signals were collimated and focused onto the entrance slit of a monochromator with the output plane equipped with a photomultiplier tube (HORIBA HuoroMax-4P). Two-photon absorption (TPA) cross sections (δ) of the samples were obtained by two-photon excited fluorescence (TPEF) method [9] at femtosecond laser pulse and Ti: sapphire system (680–1080 nm, 80 MHz, 140 fs) as the light source.

2.2. Synthesis

2.2.1. Synthesis of dye 1 (Scheme 1)

t-BuOK (1.2 g, 10 mmol) and 4-(1, 4, 7, 10-tetraoxa-13-aza-cyclopentadecyl) benzaldehyde (1 g, 3 mmol) were placed into a dry mortar and milled vigorously for about 90 min under infrared



Scheme 1. Preparation of the dyes 1 and 2.

Table 1
Photophysical properties of dye 1 and dye 2 in four different polar solvents.

Ligand	Solvents	$\lambda_{\text{max}}^{\text{a}}$	$\lambda_{\text{max}}^{\text{b}}$	ϕ^{c}	$\Delta\nu^{\text{d}}$
Dye 1	Benzene	395	455,482	0.373	3338.43
	DCM	395	494	0.361	5073.54
	THF	395	485	0.367	4697.90
	DMF	398	511	0.333	5306.15
Dye 2	Benzene	391	458, 479	0.372	3741.39
	DCM	392	489	0.368	5018.40
	THF	393	482	0.370	4698.40
	DMF	393	511	0.330	5875.82

^a Peak position of the longest absorption band.

^b Peak position of SPEF, excited at the absorption maximum.

^c Quantum yields determined by using quinine sulfate as standard.

^d Stokes' shift in cm^{-1} .

ray lamp, in the process, 4, 4-Bis(diethylphosphonomethyl) biphenyl (1.36 g, 3.0 mmol) was added in batches. After completion of the reaction (monitored by Thin Layer chromatography (TLC)), the mixture was dissolved in Dichloromethane (150 mL). The residual solid was filtered and filtrate was concentrated. Yellow-green needle product (1.24 g, 1.565 mmol) was obtained by recrystallized from dichloromethane. Yield: 52.3%. mp 233 °C; ^1H NMR (400 MHz, CDCl_3 , TMS) (Fig. S1): δ 7.59 ($J = 8$, d , 4H), 7.53 ($J = 8$, d , 4H), 7.40 ($J = 8$, d , 4H), 7.07 ($J = 16$, d , 2H), 6.92 ($J = 16$, d , 2H), 6.66 ($J = 8$, d , 4H), 3.78–3.76 (m , 8H), 3.67–3.64 (m , 32H). ^{13}C NMR (100 MHz, CDCl_3 , TMS) (Fig. S2): δ 146.25, 137.87, 136.16, 127.68, 126.80, 125.87, 125.37, 124.24, 122.60, 110.54, 70.32, 69.21, 69.15, 67.54, 51.55. IR (KBr): 3054 (m), 1610 (m), 1486 (s), 1208 (s), 1142 (s). MS (ESI): 397.22 [($M+2$)/2] $^+$. Anal. Calcd for $\text{C}_{48}\text{H}_{60}\text{N}_2\text{O}_8$: C, 72.70; H, 7.63; N, 3.53%. Found: C, 72.35; H, 7.28; N, 3.26%.

2.2.2. Synthesis of dye 2 (Scheme 1)

Dye 2 was obtained as orange powders in 40.6% yield by following a similar procedure of Dye 1. mp 207 °C; ^1H NMR (400 MHz, CDCl_3 , TMS) (Fig. S3): δ 7.59 ($J = 8$, d , 4H), 7.53 ($J = 8$, d , 4H), 7.39 ($J = 8$, d , 4H), 7.06 ($J = 16$, d , 2H), 6.92 ($J = 16$, d , 2H), 6.68 ($J = 8$, d , 4H), 3.72–3.70 (m , 8H), 3.67–3.64 (m , 40H). ^{13}C NMR (100 MHz, CDCl_3 , TMS) (Fig. S4): δ 147.58, 138.90, 137.17, 130.21, 127.84, 127.10, 126.90, 126.40, 123.62, 111.71, 70.81, 70.74, 68.72, 62.26, 62.19, 51.24. IR (KBr): 3038 (m), 1610 (m), 1491 (s), 1197 (s), 1122 (s). MS (ESI): 441.25 [($M+2$)/2] $^+$. Anal. Calcd for $\text{C}_{52}\text{H}_{68}\text{N}_2\text{O}_{10}$: C, 70.88; H, 7.78; N, 3.18%. Found: C, 71.12; H, 7.53; N, 3.31%.

2.2.2.1. Linear absorption and single-photon excited fluorescence (SPEF). The photophysical properties of dyes 1 and 2 are summarized in Table 1. The linear absorption spectra (one-photon

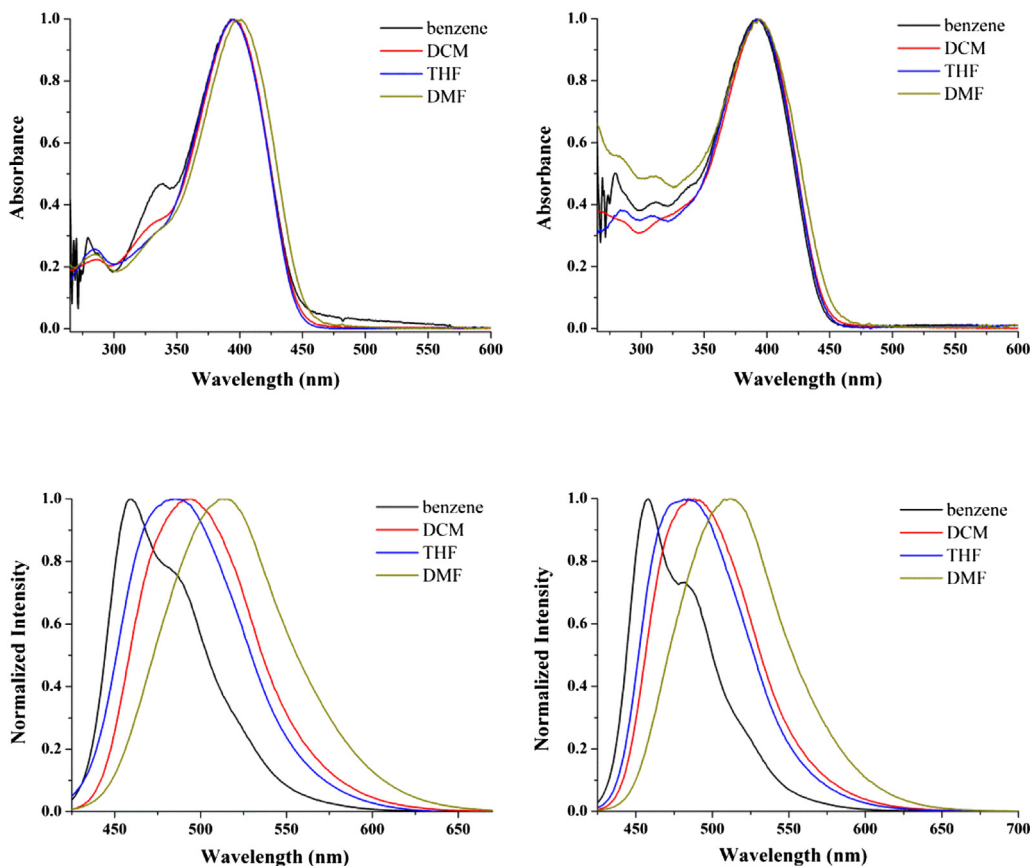


Fig. 1. Linear absorption and fluorescence of dye 1 (left) and dye 2 (right) in four organic solvents of different polarities.

absorption (OPA)) were measured in solvents of different polarities at a concentration of $1 \times 10^{-5} \text{ mol L}^{-1}$, in which influence of the solvent has been excluded. The one-photon-excited fluorescence (OPEF) spectra were measured with the same concentrations as those of the linear absorption spectra.

As shown in Fig. 1, we can see that strong absorption peaks fall in 390 nm nearby region, and weak absorption peaks fall in 300 nm nearby region. According to the density functional theory (DFT) calculations (Fig. 2), these peaks can be belong to $\pi-\pi^*$ transition of aromatic ring system [10]. DFT calculations were carried out using Gaussian 03 program. The nonlocal density function of B3LYP with 6-31G basis sets was used for the calculations [11].

The OPA spectra of dyes 1 and 2 exhibit almost no red-shift with the increasing of solvent polarity, which show negligible solvatochromic behavior. Upon increasing polarity of the solvent, as shown in Fig. 1 and Table 1, the fluorescent emission peaks of dyes 1 and 2 show remarkable bathochromic shifts and the Stokes shifts also show a tendency to monotonically increase. This can be explained by the fact that the excited state may possess a higher polarity than the ground state. An increased dipole–dipole interaction between the solute and solvent leads to a lowering of the energy level of the excited state [12,13]. Normalized UV absorption spectra in ethanol solvent are special (Fig. S5), there is a marked hypochromatic shift. It may be that the ethanol is protic solvent

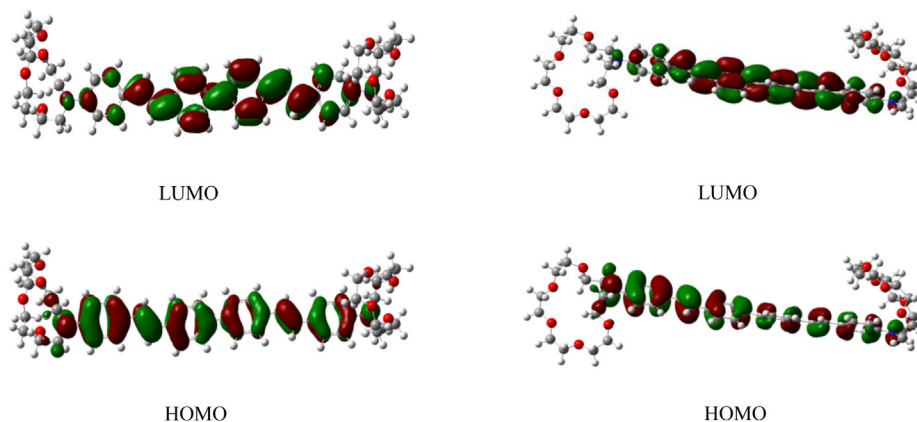


Fig. 2. Energy level and electron density distribution of frontier molecular orbitals of dye 1 (Left) and dye 2 (Right).

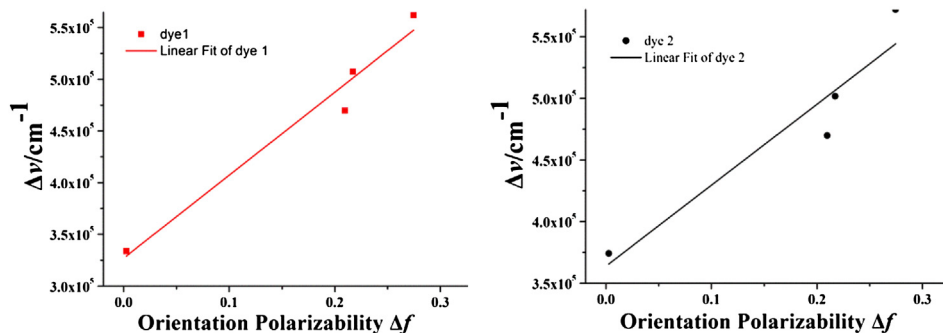


Fig. 3. Lippert–Mataga plots for dyes 1–2.

that interacts with the crown ether ring, which reduces the degree of intramolecular electron delocalization [14].

As described above, the fluorescence spectra show large Stokes shifts which depend upon the solvent polarity. Further significant solvatochromism is observed, suggesting a large change in dipole moment between the ground and emissive excited states. The Lippert–Mataga equation is the most widely used equation to evaluate the dipole moment changes of the dyes with photoexcitation [15,16] and Lippert–Mataga plots for dyes 1 and 2 are given in Fig. 3. The Lippert–Mataga equation is as follow:

$$\Delta\nu = \frac{2\Delta f}{4\pi\epsilon_0\hbar c a^3} (\mu_e - \mu_g)^2 + b$$

$$\Delta f = \frac{\epsilon - 1}{2\epsilon + 1} - \frac{n^2 - 1}{2n^2 + 1}$$

in which $\Delta\nu = \nu_{\text{abs}} - \nu_{\text{em}}$ stands for Stokes shift, ν_{abs} and ν_{em} are absorption and emission frequency (cm^{-1}), h is the Planck's constant, c is the velocity of light in vacuum, a is the Onsager radius and b is a constant. Δf is the orientation polarizability, ϵ is the refractive index, n is the dielectric constant, μ_e and μ_g are the dipole moments of the emissive and ground states, respectively and ϵ_0 is the permittivity of the vacuum. $(\mu_e - \mu_g)^2$ is proportional to the slope of the Lippert–Mataga plot.

The large slopes of dyes 1 and 2 shown in the Lippert–Mataga plot infer large dipole moment changes for dyes 1 and 2 with photoexcitation [16]. The slope of the best-fit line is related to the dipole moment change between the ground and excited states ($\mu_e - \mu_g$). The values of $\mu_e - \mu_g$ were calculated as 18.72 D for dye 1 and 16.76 D for dye 2. The large values of dyes 1 and 2 indicate that the molecule in the excited state has an extremely polar structure,

corresponding with their linear and nonlinear optical properties [17].

Photographs of solutions containing dye 1 are displayed in Fig. 4, from which one can clearly see dye 1 presents different colors in different solvents under the irradiation of ultraviolet light with 365 nm. Chromaticity coordinates [18] figure shows the distribution of the different color areas in parallel. The great sensitivity to every solvents exhibits potential and useful application for the development of efficient sensors for the detection of volatile organic compounds (VOCs) [19].

The fluorescence quantum yields (Φ) were determined by using quinine sulfate as the reference according to the literature method [20]. Quantum yields is corrected as follows.

$$\Phi_s = \Phi_r \frac{A_r \eta_s^2 D_s}{A_s \eta_r^2 D_r}$$

where the s and r indices designate the sample and reference samples, respectively, A is the absorbance at λ_{exc} , η is the average refractive index of the appropriate solution, and D is the integrated area under the corrected emission spectrum [21].

Time-resolved fluorescence measurements were performed in Fig. 5 and the detailed data of the fluorescence decay curves of dyes 1 and 2 are listed in Table 2. The decays were analyzed by the 'least-squares' method. The quality of the exponential fits was evaluated by the goodness of fit (χ^2). The experimental errors were estimated to be $\pm 15\%$ from sample concentrations and instruments. The mean excited-state lifetime (τ) of dyes 1 and 2 became longer with the increasing of the polarity of the solvents in general trend except in ethanol (Fig. S6 and Table S1), which could be explained by the hydrogen bonds between solute and ethanol molecules consume

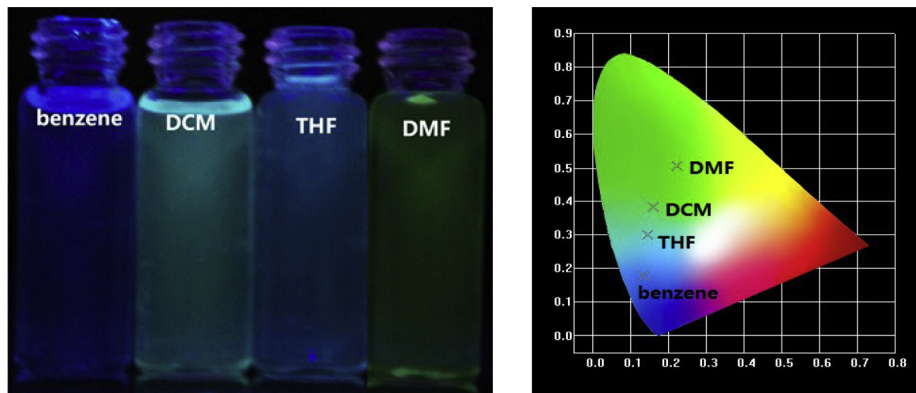


Fig. 4. The photographs of dye 1 in four solvents (benzene, DCM, THF and DMF) under the irradiation of 365 nm wavelength and chromaticity coordinates figures of dye 1.

Table 2
Fluorescence lifetimes of dyes 1 and 2 in different solvents.

Sample	λ_{det}^a (nm)	τ_1^b (ns)	A_1^c	τ_2^b (ns)	A_2^c	τ_3^b (ns)	A_3^c	$\langle\tau\rangle^d$ (ns)	χ^2
Dye1-benzene	395	0.75	0.94	1.56	0.06			0.7986	1.41
Dye1-DCM	395	0.92	0.37	1.24	0.63			1.1216	0.868
Dye1-THF	395	0.98	0.26	1.64	0.55	0.29	0.19	1.2119	1.07
Dye1-DMF	398	0.63	0.15	1.50	0.85			1.3695	1.17
Dye2-benzene	391	0.79	0.96	1.78	0.04			0.8296	1.54
Dye2-DCM	392	0.70	0.32	1.30	0.68			1.108	1.25
Dye2-THF	393	0.55	0.33	1.61	0.67			1.2536	1.09
Dye2-DMF	393	0.68	0.29	1.61	0.71			1.3403	1.03

^a Detection wavelength.
^b Fluorescence lifetime.
^c Fractional contribution.
^d Weighted mean lifetime.

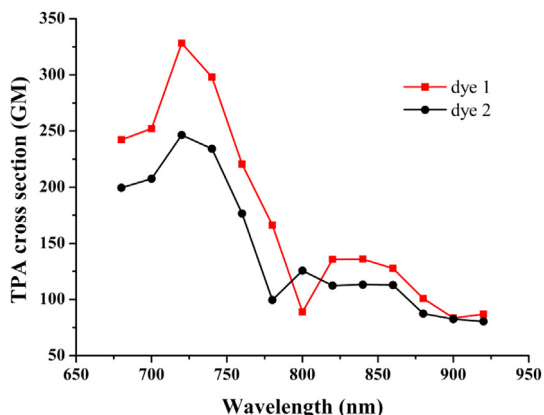


Fig. 8. Two-photon absorption cross sections of dyes 1 and 2 (chloroform solution 10^{-3} M) in 680–920 nm regions.

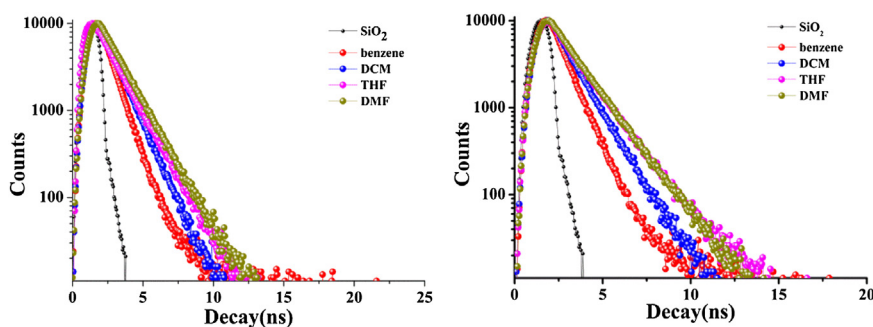


Fig. 5. The normalized fluorescence lifetimes at $\lambda_{ex} = 395$ nm for dye 1 (Left) and dye 2 (Right) in four solvents.

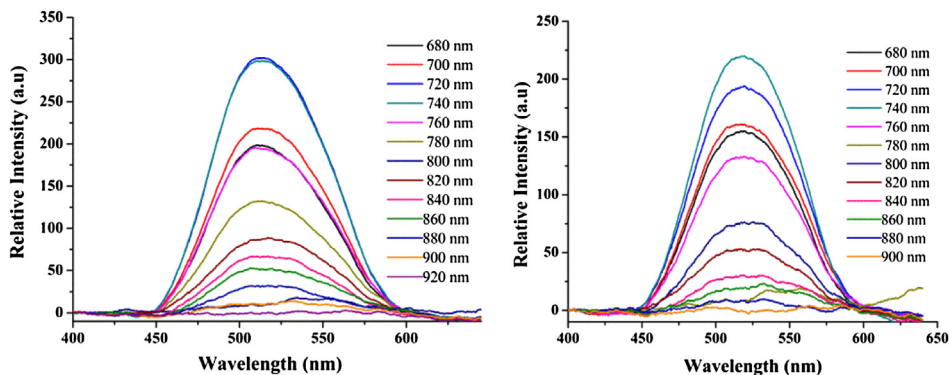


Fig. 6. The TPEF spectra of dye 1 (Left) and dye 2 (Right) in $CHCl_3$ pumped by femtosecond laser pulses at 300 mw under different excitation wavelengths (1×10^{-3} mol L^{-1}).

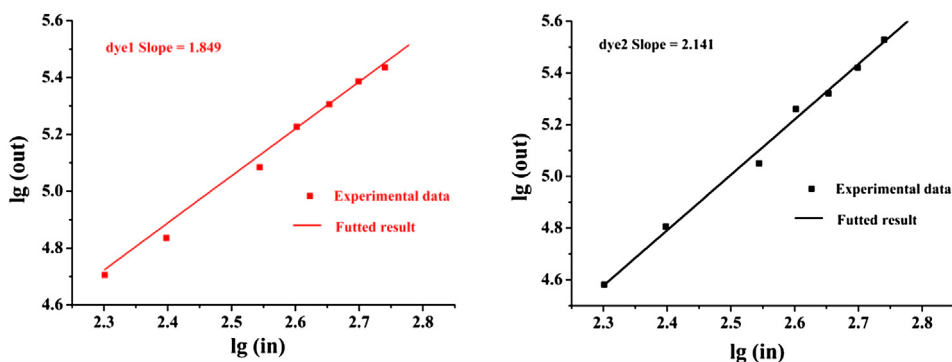


Fig. 7. Output fluorescence intensity (I_{out}) vs. the square of input laser power (I_{in}) for dye 1 (Left) and dye 2 (Right), excitation carried out at 740 nm, with $c = 1 \times 10^{-3}$ mol/L in $CHCl_3$.

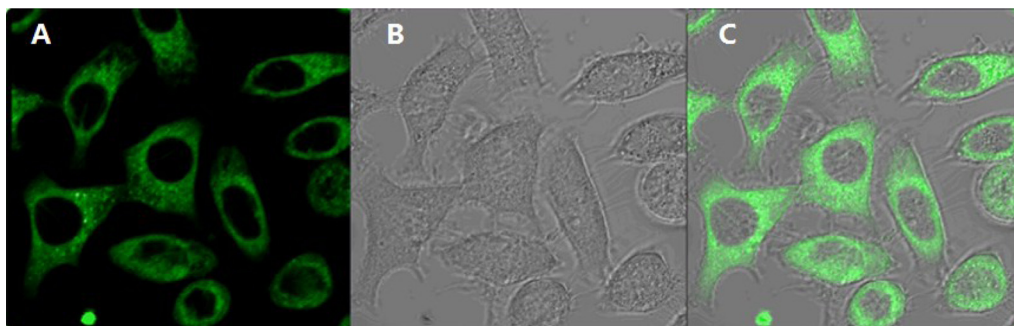


Fig. 9. (A) single-photon fluorescence microscopy (SPFM) image of HepG2 cells with excitation at 511 nm. (B) Bright-field image of HepG2 cells stained with dye1. (C) Merged image.

some energy from the excited state molecules [22]. The lifetimes (τ) of dyes 1 and 2 decay as a tripple exponential in ethanol, while in other four solvents the mean lifetime (τ) are mainly the result of combined action of single-exponential and double-exponential.

In the wavelength range 450–900 nm, there is no linear absorption for the dyes, which indicates that there are no molecular energy levels corresponding to an electron transition in the spectral range. In test process, laser induced frequency up-converted fluorescence in this spectral range appeared, which can be ascribed to two-photon-excited fluorescence (TPEF). Upon excitation from 450 to 920 nm, it is impossible to produce single-photon-excited up-converted fluorescence. From Fig. 6, we can conclude that the optimum excitation wavelength of dyes 1 and 2 are not associated with the laser energy, but the two-photon fluorescence intensity is associated with excitation wavelength, the optimal excitation wavelength of two dyes is 740 nm. Dyes 1 and 2 in CHCl_3 were pumped by femtosecond laser pulses at different pump intensities with 740 nm excitation wavelength. Fig. 7 shows a log–log plot of the excited fluorescence signal vs. excited light power [23]. The slope value is 1.849 for dye 1 and 2.141 for dye 2, respectively. It provides direct evidence for the squared dependence of excited fluorescence intensity and input laser power, suggesting a two-photon excitation mechanism.

TPA cross sections (δ) of samples is determined by Eq.:

$$\delta = \delta_{\text{ref}} \frac{\Phi_{\text{ref}} c_{\text{ref}} n_{\text{ref}} F}{\Phi c n F_{\text{ref}}}$$

where the 'ref' subscript represents the reference molecule (here fluorescein in aqueous solution of sodium hydroxide at a concentration of $1.0 \times 10^{-3} \text{ mol L}^{-1}$ was used as the reference). δ is the TPA cross-sectional value, c is the concentration of the solution, n is the refractive index of the solution, F is the TPEF integral intensities of the solution emitted at the exciting wavelength, and Φ is the fluorescence quantum yield. The δ_{ref} value of reference was taken from the literature [24]. Two-photon absorption cross sections of dyes 1 and 2 in 680–920 nm region are displayed in Fig. 8. The two-photon absorption cross sections of dyes 1 and 2 are 328.2 GM and 246.55 GM in 740 nm, respectively, which are in good agreement with the calculated values of dipole moment.

2.2.2.2. Application of dye 1 for single-photon microscopy bio-imaging. To evaluate the performance of dye 1 in living cells, single- and two-photon fluorescence microscopy (SPFM and TPFM) imaging is performed in Fig. 9. HepG2 cells were the testing candidates and were cultured and stained with dye 1. A bright-field image of each cell was taken immediately prior to the SPFM imaging. The SPFM image and the merged image show that after 2 h incubation with HepG2 cells, dye 1 went through the membrane and localized uniformly in the cytoplasm. The intense fluorescence

is mainly a result of dye 1 internalized in the HepG2 cell cytoplasm and the distribution in the nucleolus is significantly lower, suggesting that only the cell cytoplasm can be labeled by dye 1. These results demonstrate the potential bio-imaging applications of dye 1 by labeling HepG2 cells. However, two-photon fluorescence microscopy (TPFM) imaging was not performed successfully in DMSO, the TPEF spectra of dyes 1 and 2 were tested in CHCl_3 rather than DMSO because of the poor solubility of the dyes in DMSO.

3. Conclusions

In this contribution, two novel aza-crown ether derivatives based on stilbene compounds with moderate two-photon absorption cross sections were synthesized. Photophysical properties and the two-photon fluorescence microscopy (TPFM) were systematically investigated. The two dyes exhibited positive solvatochromic properties in various solvents mainly due to the $\pi-\pi^*$ transition of aromatic ring system, which are in line with DFT calculations. The solvatochromic behavior of dye 1 offers potential application in the detection of volatile organic compounds (VOCs). Moreover, we also demonstrated that dye 1 had the potential for application in single-photon fluorescence imaging.

Acknowledgments

This work was supported by the Program for New Century Excellent Talents in University (China), the Doctoral Program Foundation of the Ministry of Education of the People's Republic of China (20113401110004), the National Natural Science Foundation of China (21271003, 21271004 and 51372003), the Ministry of Education of the People's Republic of China, the Natural Science Foundation of Education Committee of Anhui Province (KJ2012A024), the Natural Science Foundation of Anhui Province (1208085MB22), the 211 Project of Anhui University, the Ministry of Education Funded Projects Focus on Returned Overseas Scholar.

Appendix A. Supplementary data

Supplementary data related to this article can be found at <http://dx.doi.org/10.1016/j.dyepig.2014.03.034>.

References

- [1] (a) Pawlicki M, Collins HA, Denning RG, Anderson HL. Two-photon absorption and the design of two-photon dyes. *Angew Chem Int Ed* 2009;48(18):3244–66; (b) Terenzi F, Katan C, Badaeva E, Tretiak S, Blanchard-Desce M. Enhanced two-photon absorption of organic chromophores: theoretical and experimental assessments. *Adv Mater* 2008;20(24):4641–78.
- [2] (a) Li K, Liu Y, Pu KY, Feng SS, Zhan R, Liu B. Polyhedral oligomeric silsesquioxanes-containing conjugated polymer loaded PLGA nanoparticles with trastuzumab (Herceptin) functionalization for HER2-positive cancer cell detection. *Adv Funct Mater* 2011;21(2):287–94;

- (b) Goswami TK, Gadadhar S, Roy M, Nethaji M, Karande AA, Chakravarty AR. Ferrocene-conjugated copper (II) complexes of L-methionine and phenanthroline bases: synthesis, structure, and photocytotoxic activity. *Organometallics* 2012;31(8):3010–21;
- (c) Tian H, Feng Y. Next step of photochromic switches? *J Mater Chem* 2008;18(14):1617–22;
- (d) Lin T-C, Huang Y-J, Chen Y-F, Hu C-L. Two-photon absorption and effective broadband optical power limiting properties of a multi-branched chromophore containing 2, 3-diarylquinoxalinylium moieties as the electron-pulling units. *Tetrahedron* 2010;66(6):1375–82;
- (e) LaFratta CN, Fourkas JT, Baldacchini T, Farrer RA. Multiphoton fabrication. *Angew Chem Int Ed* 2007;46(33):6238–58.
- [3] (a) Strehmel B, Strehmel V. Two-photon physical, organic and polymer chemistry: theory, techniques, chromophore design, and applications. *Adv Photochem* 2007;29:111–354;
- (b) Rumi M, Barlow S, Wang J, Perry JW, Marder SR. Two-photon absorbing materials and two-photon-induced chemistry. *Photoresponsive polymers I*. Springer; 2008. pp. 1–95;
- (c) Terenziani F, Katan C, Badaeva E, Tretiak S, Blanchard-Desce M. Enhanced two-photon absorption of organic chromophores: theoretical and experimental assessments. *Adv Mater* 2008;20(24):4641–78;
- (d) Kim HM, Seo MS, Jeon S-J, Cho BR. Two-photon absorption properties of hexa-substituted benzene derivatives. Comparison between dipolar and octupolar molecules. *Chem Commun* 2009;47:7422–4;
- (e) Pawlicki M, Collins HA, Denning RG, Anderson HL. Two-photon absorption and the design of two-photon dyes. *Angew Chem Int Ed* 2009;48(18):3244–66;
- (f) Liu Z, Shao P, Huang Z, Liu B, Chen T, Qin J. Two-photon absorption enhancement induced by aggregation due to intermolecular hydrogen bonding in V-shaped 2-hydroxypyrimidine derivatives. *Chem Commun* 2008;(19):2260–2.
- [4] (a) Reinhardt BA, Brott LL, Clarson SJ, Dillard AG, Bhatt JC, Kannan R, et al. Highly active two-photon dyes: design, synthesis, and characterization toward application. *Chem Mater* 1998;10(7):1863–74;
- (b) Belfield KD, Hagan DJ, Van Stryland EW, Schafer KJ, Negres RA. New two-photon absorbing fluorene derivatives: synthesis and nonlinear optical characterization. *Org Lett* 1999;1(10):1575–8.
- [5] Belfield KD, Schafer KJ, Mourad W, Reinhardt BA. Synthesis of new two-photon absorbing fluorene derivatives via Cu-mediated Ullmann condensations. *J Org Chem* 2000;65(15):4475–81.
- [6] Kim O-K, Lee K-S, Woo HY, Kim K-S, He GS, Swiatkiewicz J, et al. New class of two-photon-absorbing chromophores based on dithienothiophene. *Chem Mater* 2000;12(2):284–6.
- [7] (a) Albota M, Beljonne D, Brédas J-L, Ehrlich JE, Fu J-Y, Heikal AA, et al. Design of organic molecules with large two-photon absorption cross sections. *Science* 1998;281(5383):1653–6;
- (b) Rumi M, Ehrlich JE, Heikal AA, Perry JW, Barlow S, Hu Z, et al. Structure-property relationships for two-photon absorbing chromophores: bis-donor diphenylpolyene and bis (styryl) benzene derivatives. *J Am Chem Soc* 2000;122(39):9500–10.
- [8] (a) Araya R, Andino-Pavlovsky V, Yuste R, Etchenique R. Two-photon optical interrogation of individual dendritic spines with caged dopamine. *ACS Chem Neurosci* 2013;4(8):1163–7;
- (b) Arunkumar E, Fu N, Smith BD. Squaraine-derived rotaxanes: highly stable, fluorescent near-IR dyes. *Chem A Eur J* 2013;4(8):4684–90.
- [9] Lee SK, Yang WJ, Choi JJ, Kim CH, Jeon S-J, Cho BR. 2, 6-Bis [4-(p-dihexylaminostyryl) styryl] anthracene derivatives with large two-photon cross sections. *Org Lett* 2005;7(2):323–6.
- [10] Yong C-S, Bie G-J, Xu X-J, Chin J. *Luminescence* 2008;5:815–20.
- [11] (a) Xu Q-Q, Wang D-H, Chi S-M, Gan X, Fu W-F. Synthesis, structures and spectroscopic properties of platinum (II), copper (I) and zinc (II) complexes bearing 4-(p-dimethylaminophenyl)-6-phenyl-2, 2'-bipyridine ligand. *Inorg Chim Acta* 2009;362(8):2529–36;
- (b) Lippert E, Rettig W, Bonacic-Koutecky V, Heisel F, Miehle J. Photophysics of internal twisting. *Adv Chem Phys* 1987;68(1).
- [12] Fromherz P. Monopole-dipole model for symmetrical solvatochromism of hemicyanine dyes. *J Phys Chem* 1995;99(18):7188–92.
- [13] Narang U, Zhao CF, Bhawalkar JD, Bright FV, Prasad PN. Characterization of a new solvent-sensitive two-photon-induced fluorescent (aminostyryl) pyridinium salt dye. *J Phys Chem* 1996;100(11):4521–5.
- [14] Ito M, Inuzuka K, Imanishi S. Effect of solvent on n- π^* absorption spectra of Ketones. *J Am Chem Soc* 1960;82(6):1317–22.
- [15] Patel SA, Cozzuol M, Hales JM, Richards CI, Sartin M, Hsiang J-C, et al. Electron transfer-induced blinking in Ag nanodot fluorescence. *J Phys Chem C* 2009;113(47):20264–70.
- [16] Ji S, Yang J, Yang Q, Liu S, Chen M, Zhao J. Tuning the intramolecular charge transfer of alkynylpyrenes: effect on photophysical properties and its application in design of OFF–ON fluorescent thiol probes. *J Org Chem* 2009;74(13):4855–65.
- [17] Irie M, Sayo K. Solvent effects on the photochromic reactions of diarylethene derivatives. *J Phys Chem* 1992;96(19):7671–4.
- [18] Broadbent D. A critical review of the development of the CIE1931 RGB color-matching functions. *Color Res Appl* 2004;29(4):267–72.
- [19] (a) Sathiamoorthy G, Kalyana S, Finney W, Clark R, Locke B. Chemical reaction kinetics and reactor modeling of NO_x removal in a pulsed streamer corona discharge reactor. *Indust Eng Chem Res* 1999;38(5):1844–55;
- (b) Evans D, Rosocha LA, Anderson GK, Coogan JJ, Kushner MJ. Plasma remediation of trichloroethylene in silent discharge plasmas. *J Appl Phys* 1993;74(9):5378–86.
- [20] Crosby GA, Demas JN. Measurement of photoluminescence quantum yields. *Review. J Phys Chem* 1971;75(8):991–1024.
- [21] Gray TG, Rudzinski CM, Meyer EE, Holm R, Nocera DG. Spectroscopic and photophysical properties of hexanuclear rhenium (III) chalcogenide clusters. *J Am Chem Soc* 2003;125(16):4755–70.
- [22] (a) Ryan CJ, Elmes RB, Quinn SJ, Gunnlaugsson T. Synthesis and photophysical evaluations of fluorescent quaternary bipyridyl-1, 8-naphthalimide conjugates as nucleic acid targeting agents. *Supramol Chem* 2012;24(3):175–88;
- (b) Elmes RB, Orange KN, Cloonan SM, Williams DC, Gunnlaugsson T. Luminescent ruthenium (II) polypyridyl functionalized gold nanoparticles; their DNA binding abilities and application as cellular imaging agents. *J Am Chem Soc* 2011;133(40):15862–5;
- (c) Robson KC, Koivisto BD, Gordon TJ, Baumgartner T, Berlinguette CP. Triphenylamine-modified ruthenium (II) terpyridine complexes: enhancement of light absorption by conjugated bridging motifs. *Inorg Chem* 2010;49(12):5335–7.
- [23] Denk W, Strickler JH, Webb WW. Two-photon laser scanning fluorescence microscopy. *Science* 1990;248(4951):73–6.
- [24] Xu C, Webb WW. Measurement of two-photon excitation cross sections of molecular fluorophores with data from 690 to 1050 nm. *JOSA B* 1996;13(3):481–91.